Simulation of Formwork Filling by Cement Fluid: the Effect of the Formwork Structure on Yield-stress Fluid

Mehrdad Alfi[1], Nilanjana Benarjee[1], Dimitri Feys[2], and Joontaek Park[*1]
[1]Chemical and Biochemical Engineering Department, Missouri University of Science & Technology, Rolla, MO, USA
[2]Civil, Architectural & Environmental Engineering Department, Missouri University of Science & Technology, Rolla, MO, USA
*Corresponding author: 143 Schrenk Hall, 400 W 11th St, Missouri S&T, Rolla, MO, 65409, USA, parkjoon@mst.edu

Abstract: The flow of Self-Consolidating Concrete (SCC) in formwork fillings was simulated as the flow of a single phase yield-stress fluid between two infinite plates by COMSOL Multiphysics®. The flow of SCC with varied rheological properties (yield stress and plastic viscosity) was verified in formworks with different configurations of reinforcement (rebars), such as the distance between the rebars and the wall and the separation distance between the rebars. Minimum and maximum limits of SCC rheological properties in each configuration were identified to avoid the presence of a dead zone, which was identified as an unyielded zone with low flow velocity. The simulation results showed that the occurrence of the dead zones was less likely in the configurations with a larger distance between the rebars or with a larger distance between rebar and the wall. In other words, concrete with lower plastic viscosity and higher yield stress can be used in such configurations with reduction of the energy requirement for placing.

Keywords: Self-consolidating concrete, concrete flow, yield-stress fluid

1. Introduction

In this study, COMSOL Multiphysics® was used to simulate the flow of Self-Consolidating Concrete (SCC) in formworks. Limiting values for the rheological properties of concrete, for which the occurrence of construction defects is likely, were investigated in relation to the formwork configuration.

Self-Consolidating Concrete is a relatively new type of concrete which does not require any energy for consolidation [1]. Consequently, the hardened properties of the cast structural element are largely influenced by the flow pattern of SCC in the formwork [2]. Several examples are available in literature showing the existence of dead zones, dynamic segregation induced by high shear rates, filling of formworks as a function of the concrete yield stress, lower mechanical properties due to multi-layer casting, etc.

The occurrence of dead zones during formwork filling induces lower mechanical properties and durability of the final structural elements. In literature, it is shown that the volume of entrapped air increases in dead zones. As a result, the local concrete strength is significantly decreased [3]. Dead zones also increase the risk of casting joints or cold joints, reducing the bond strength between the concrete layers [2]. For conventional vibrated concrete, these problems are avoided by the application of vibration energy. As for SCC, vibration is prohibited [1], a more detailed investigation of the formwork filling is necessary to avoid these dead zones.

Instead of performing large-scale experiments with large quantities of concrete, the flow in formworks can also be predicted by means of numerical, single fluid simulations, in which the concrete is assumed to be a fluid without particles. However, numerical simulations that take into consideration the influence of reinforcement (rebars) on local patterns in SCC flow have not been reported extensively. Preliminary simulations have shown that a vertical bar creates additional zones with very low and very high shear rates, compared to the flow in non-reinforced elements [4].

In this study, the flow of SCC in a formwork filling was simulated as a single phase yield-stress fluid in a channel which has cylindrical objects in it. The focus was put on avoiding the

dead zones where the concrete is at rest and entrapped air bubbles are less likely to evacuate, reducing the mechanical properties of the concrete. The influence of reinforcement on the flow of SCC in a formwork was studied. Four different rebar configurations were chosen in terms of concrete cover (distance between rebar and wall) and the distance between the rebars in flow direction. The concrete cover is an important parameter for the durability of the structural element while the distance between the rebars is determined based on the loading of the structural element. Both parameters are fixed when designing structures [5]. As a result, only the concrete rheological properties can be varied to avoid the occurrence of dead zones. For each configuration, the rheological properties (plastic viscosity and yield stress) of the SCC flow were optimized for good formwork filling. In other words, the goal is to find the optimum plastic viscosity and yield stress to ensure no dead zones and the still provide adequate formwork filling.

2. Governing Equations

Since the SCC flow is simulated as a single phase incompressible yield-stress fluid in a laminar flow regime, the governing equations are the continuity equation and the Cauchy momentum balance equation (ρ: fluid density, **u**: fluid velocity vector, t: time, p: pressure, $\boldsymbol{\tau}$: stress tensor, and **g**: gravity acceleration vector).

$$\frac{\partial \rho}{\partial t} = -\nabla \cdot (\rho \boldsymbol{u}) \qquad (1)$$

$$\rho \frac{D\boldsymbol{u}}{Dt} = -\nabla p + \nabla \cdot \boldsymbol{\tau} + \rho \boldsymbol{g} \qquad (2)$$

In this study, the yield-stress fluid is modeled as Bingham fluid. Therefore, the constitutive equation for $\boldsymbol{\tau}$ in (2) is given in terms of plastic viscosity, μ_p, yield stress, τ_y, correction parameter, ε, deformation tensor, $\Delta = \nabla \mathbf{u} + (\nabla \mathbf{u})^T$, and shear rate, $\dot{\gamma} = \sqrt{\frac{1}{2}\Delta : \Delta}$.

$$\boldsymbol{\tau} = \left(\mu_p + \frac{\tau_y}{\dot{\gamma} + \varepsilon}\right)\Delta \qquad (3)$$

Note here that ε is commonly used for numerical simulation of Bingham fluid to avoid the singularity of (3) by imposing a minimum shear rate [6].

3. Methods

3.1 Parameters

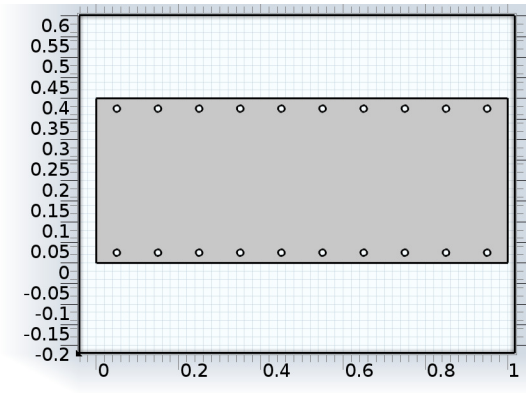

Figure 1. A formwork configuration (Case A-1)

An example of a formwork configuration in this study is demonstrated in Figure 1. Formwork is simulated as a channel with its length of 1 m and its height of 0.4 m. The circular objects, with a constant diameter of 0.016 m, near each wall represent the rebars. The nearest distance between the center of a rebar and a wall, d_w, as well as the distance between the centers of rebars in flow direction, d_p, are varied for each case. Table 1 summarizes the rebar configuration and description of each case. Case A is for investigating the effect of d_w and Case B is for the effect of d_p.

Cases	d_w (m)	d_p (m)	Description
Case A-1	0.025	0.1	Small d_w
Case A-2	0.05	0.1	Large d_w
Case B-1	0.0375	0.05	Small d_p
Case B-2	0.0375	0.25	Large d_p

Table 1. Rebar configuration and description of each case

Both the inlet and the outlet average flow rates are set to U_i=U_o=0.1 m/s with both the entrance as well as the outlet lengths of 0.3 m to

ensure a fully-developed flow. Boundary conditions of all the solid surfaces of the walls and rebars are the no-slip boundary conditions.

The fluid density of the SCC flow is chosen as 2350 kg/m^3. The viscosity, μ, of Bingham fluid can be simulated by using the user-defined model with (3). The rheological properties (μ_p and τ_y) are chosen as described in section 3.3. The values of ε are estimated to ensure the maximum fluid viscosity of 10^6 Pa.s for each rheological parameters.

Triangular mesh is used for the whole domain. A total of 10382 elements was created using the physically-controlled coarse mesh. The default solver is used with the maximum iteration of 300, which was enough for getting convergent solutions in this study.

3.2 Identifying 'Dead Zone'

The dead zone is identified as the unyielded zone with low velocity in this simulation. The 2D maps of the dimensionless velocity, $u^*=u/U_i$ and the dimensionless stress, $\tau^* = (\mu\dot{\gamma})/\tau_y$, are plotted to be used for identifying the dead zone. The region where both u* and τ* are less than 1 is considered as the dead zone. The low velocity region (u*<1) is usually found to be the region between the rebar and a wall. Therefore, an unyielded region (τ*<1) found in that region is identified as the dead zone. Adjusting the display range of the 2D map can clearly identify the unyielded zone as an empty region surrounded by dark blue regions.

3.3 Optimization of Rheological Properties

The rheological properties of SCC can be adjusted by the concrete mix down. However, μ_p and τ_y cannot be controlled precisely and individually. The possible properties range of μ_p and τ_y for SCC can be demonstrated by the rheograph, the μ_p –τ_y map [7]. In this study, the property optimization was performed along the line above the SCC zone in the rheograph, where the largest possible values of τ_y at each μ_p are located. In other words, the rheological properties must be optimized between the high μ_p and low τ_y flow and the low μ_p and high τ_y flow.

The high μ_p and low τ_y flow has a very low chance of resulting in an unyielded zone. However, high concrete viscosity increases the energy required to place the concrete. Furthermore, high viscosities slow down the self-consolidation of the concrete and can lead to lower mechanical properties due to entrapped air. On the other hand, the low μ_p and high τ_y flow has the advantage of low energy requirement for placing but has a higher chance of the occurrence of the dead zones. Therefore, finding the optimized rheological properties is important for good formwork filling. In short, the SCC flow with the maximum τ_y without dead zone is favorable.

μ_p (Pa.s)	τ_y (Pa)
100	2
90	5
80	9
70	14
60	21
50	30
40	40
30	52
20	65
10	80

Table 2. The order of rheological properties for the optimization

For each case, a simulation of the highest μ_p (=100 Pa.s) and the lowest τ_y (=2 Pa) flow is performed. Usually, the simulation results from those properties do not show any dead zone. The pressure drop between the inlet and the outlet of the channel using the line average tool is also measured. The simulations of other rheological properties, as in the order indicated in Table 2, are tried until the dead zone is identified. The sets of rheological properties in Table 2 were determined by approximating the maximum τ_y-μ_p line above the SCC zone in the rheogragh [7]. In the simulations, the rheological properties were varied according to Table 2. Once the dead zone was identified for a certain combination of τ_y and μ_p, the previous τ_y-μ_p combination with lower yield stress and higher plastic viscosity was chosen as optimum. The pressure drop at the optimized set of the properties is used to calculate the reduction in comparison with the

pressure drop resulted from the set of the highest μ_p and the lowest τ_y. Note here that this optimization procedure can be much improved by using the optimization module.

4. Results and Discussion

4.1. Case A: Effect of rebar-wall distance (d_w)

Two different cases were simulated in order to investigate the effect of d_w on the flow pattern inside the channel. In both cases, the only parameter varied is d_w, while d_p is fixed at 0.1 m: d_w = 0.025 m is for Case A-1 and d_w = 0.05 m is for Case A-2 (Table 1).

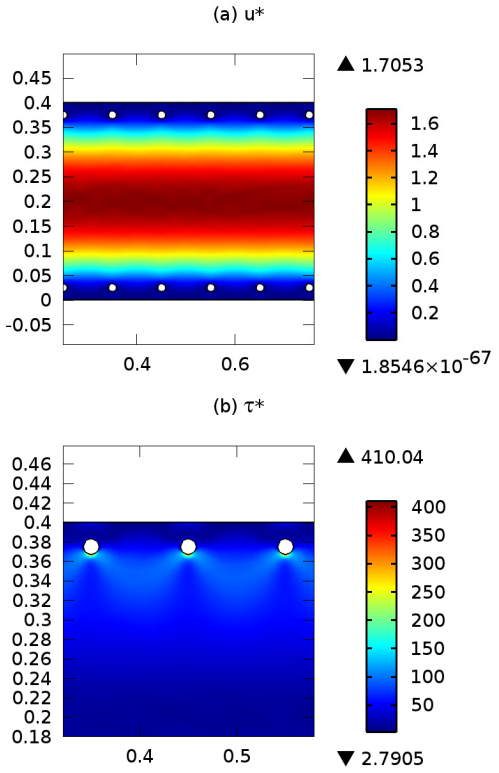

Figure 2. Simulation results of a) u* and b) τ* from Case A-1 with μ_p = 100 Pa.s and τ_y = 2 Pa.

Results from Case A-1 are shown in Figures 2~3. As described in section 3.3, the rheological property set of the highest μ_p (= 100 Pa.s) and the lowest τ_y (= 2 Pa) was investigated first. Figure 2a shows the 2D map of u*. The SCC was simulated to flow with the velocity slower than U_i near the wall and the rebars, whereas its velocity was found to be faster than U_i at the center region. Therefore, any unyielded zone near the wall and rebars would be the dead zone, as mentioned in section 3.2. However, as shown in Figure 2b, the entire area was found to have no dead zone (τ*>1). This is due to the fact that the large value of μ_p causes the values of shear stress in the entire channel to be greater than the small value of τ_y. Additionally, the pressure drop between the inlet and the outlet was measured as 1172 Pa/m.

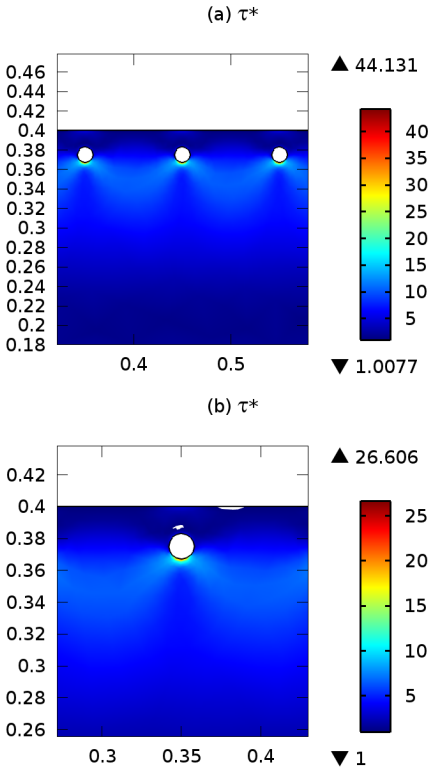

Figure 3. Simulation results of τ* from Case A-1 with a) μ_p = 70 Pa.s and τ_y = 14 Pa and b) μ_p = 60 Pa.s and τ_y = 21 Pa.

A series of simulations with different sets of the rheological properties, as indicated in Table 2, were also performed until the dead zone was detected. As each set, which has a trend of decreasing μ_p and increasing τ_y, was tried, the local values of τ* became lower to increase the chance of the dead zone formation. It was finally found that a set of properties with μ_p = 70 Pa.s and τ_y = 14 Pa was the optimized properties for Case A-1, as shown in Figure 3a. This means that the dead zone started to occur at the set of

properties with μ_p = 60 Pa.s and τ_y = 21 Pa, as shown in Figure 3b. The pressure drop at the optimized properties was measure as 952 Pa, which corresponds to 19% reduction in comparison to one from μ_p = 100 Pa.s and τ_y = 2 Pa. This means that the flow with smaller μ_p and larger τ_y can be used in a formwork filling with less energy required for the concrete placement. Note here that all the velocity maps rom all the cases in this study showed the same trend as in the Figure 1a. Therefore, the unyielded zones near the wall and the rebars were always considered as dead zones whereas the unyielded zone at the center of channel was not.

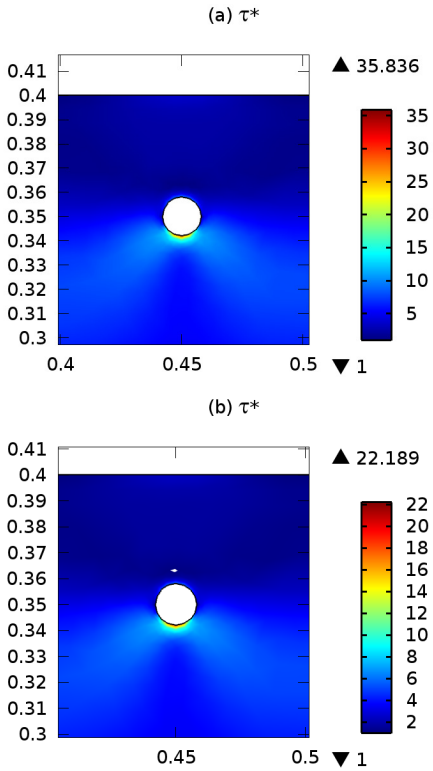

Figure 4. Simulation results of τ* from Case A-2 with a) μ_p = 60 Pa.s and τ_y = 21 Pa and b) μ_p = 50 Pa.s and τ_y = 30 Pa.

Simulations of Case A-2 were performed to investigate the effect of d_w, compared to Case A-1, which has smaller d_w. The results from Case A-2 were summarized in Figure 4. As in Case A-1, no dead zone was detected for the set of properties with μ_p = 100 Pa.s and τ_y = 2 Pa (data not shown). However, different optimized properties were found: a set of μ_p = 60 Pa.s and τ_y = 21 Pa was found to be the optimized properties (Figure 4a) because the dead zone was detected at μ_p = 50 Pa.s and τ_y = 30 Pa (Figure 4b). Furthermore, the pressure drop reduction was measured as 27%, which is greater than that of Case A-1. Therefore, these results show that for larger d_w, a lower μ_p and higher τ_y can be chosen to avoid the dead zone.

4.2. Case B: Effect of d_p

The effect of d_p on the flow pattern inside the channel was also investigated by choosing two different cases with different values of d_p. For Case B-1, d_p equals 0.05 m and for Case B-2, the value of d_p is 0.25 m while keeping d_w = 0.0375 m as constant (Table 1).

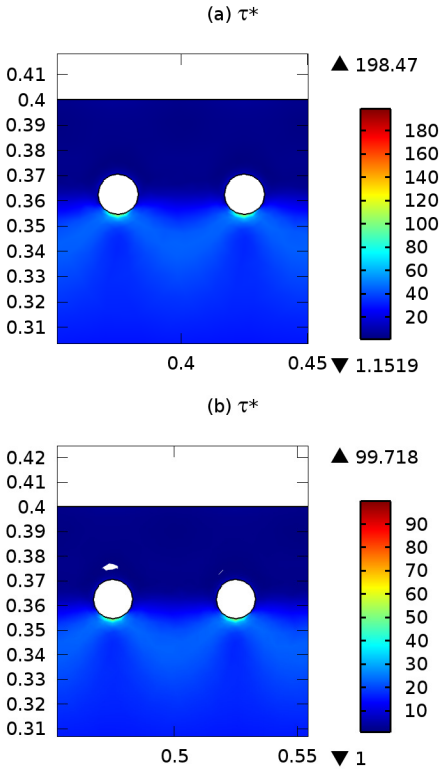

Figure 5. Simulation results of τ* from Case B-1 with a) μ_p = 90 Pa.s and τ_y = 5 Pa and b) μ_p = 80 Pa.s and τ_y = 9 Pa.

Figure 5 shows the results from the simulations of Case B-1. As described in section 3.3., the property optimization was performed by a series of simulations starting from the rheological property set of the highest μ_p (= 100

Pa.s) and the lowest τ_y (= 2 Pa). The entire domain was found to be fully sheared as in Case A (data not shown). The pressure drop at this set of the properties was found to be 1669 Pa/m. The optimized properties were found to be the set of μ_p = 90 Pa.s and τ_y = 5 Pa (Figure 5a). The dead zone was detected at the results from the set of μ_p = 80 Pa.s and τ_y = 9 Pa (Figure 5b). Since the difference between the initial set of properties and the optimized properties was found to be small, the pressure drop reduction was evaluated as only 8%.

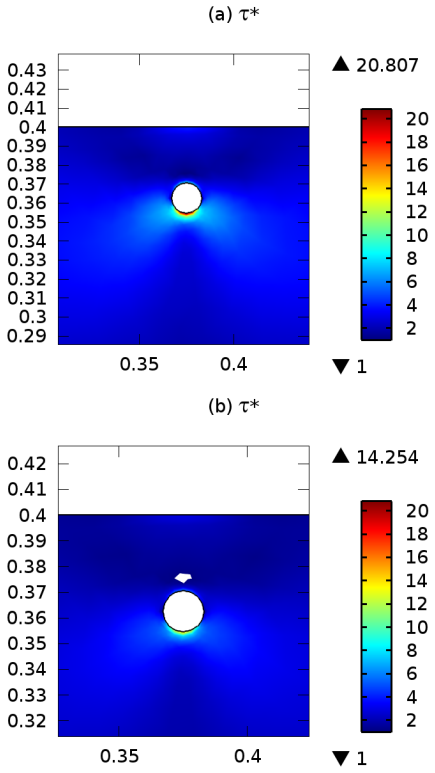

Figure 6. Simulation results of τ* from Case B-2 with a) μ_p = 50 Pa.s and τ_y = 30 Pa and b) μ_p = 40 Pa.s and τ_y = 40 Pa.

The effect of d_p was investigated by comparing the results from Case B-1 and Case B-2, which are shown in Figure 6. Starting from the set of μ_p = 100 Pa.s and τ_y = 2 Pa, which also resulted in no dead zone (data not shown), the properties were optimized at the set of μ_p = 50 Pa.s and τ_y = 30 Pa (Figure 6a). The pressure drop reduction at that property set was 24%. The dead zone was found at the results from the set of μ_p = 40 Pa.s and τ_y = 40 Pa (Figure 6b). The optimized properties and the pressure drop resulted from Case B-2 suggest that larger d_p is required to prevent the dead zone formation and reduce the energy for the concrete placement.

5. Conclusion

This study investigated the optimum rheological properties of SCC for formwork filling in presence of rebars. COMSOL Multiphysics® was used to simulate the flow pattern and the stress inside the channel for each configuration and each set of rheological properties. The properties were optimized to find the minimum μ_p and the maximum τ_y which results in no dead zone. The resulted optimized set of properties and the pressure drop reduction are summarized in Table 3. The results suggest that with increasing d_w or d_p the combination of lower μ_p and higher τ_p can be used to obtain adequate SCC flow in the formwork, Furthermore, this results in a reduction of the energy needed for the placement of concrete.

Future studies will continue to investigate the high shear rate region, which can also give construction defect due to segregation of the coarse particles, as well as the effect of other formwork configurations, such as the channel height and the rebar diameter. The optimization scheme may also be improved by choosing a different path on the rheograph with the help of the optimization module.

Cases	μ_p (Pa.S)	τ_y (Pa)	$\%\frac{\Delta P}{\Delta P_{100}}$
Case A-1	70	14	81
Case A-2	60	21	73
Case B-1	90	5	92
Case B-2	50	30	76

Table 3. Summary of the optimum rheological properties and the pressure drop reduction.

6. References

1. De Schutter G., Bartos P., Domone P., Gibbs J., *Self-Compacting Concrete*, Whittles Publishing, Caithness (2008), 296pp.

2. Roussel N., Cussigh F., “Distinct-layer casting of SCC: The mechanical consequences of thixotropy.” *Cem. Conc. Res.*, **38**, 624-632 (2008).
3. Thrane L.N., “Form Filling with Self-Compacting Concrete”, Ph-D dissertation, DTU, 2007, 295pp.
4. Roussel N., Geiker M.R., Dufour F., Thrane L.N., Szabo P., “Computational modeling of concrete flow: a general overview,” *Cem. Conc. Res*., **37**, 1298-1307 (2007).
5. ACI-318 Building Code, The American Concrete Institute (2011).
6. Denn M.M., Bonn D., “Issues in the flow of yield-stress liquids,” *Rheol. Acta*, **50**, 307-315 (2011).
7. Wallevik O. H., Wallevik J. E., “Rheology as a tool in concrete science: The use of rheographs and workability boxes,” *Cem. Conc. Res*., **41**, 1279-1288 (2011).

7. Acknowledgements

This work was supported by Center for Infrastructure Engineering Studies at Missouri S&T (RD489).